Hindawi Publishing Corporation
Advances in Materials Science and Engineering
Volume 2012, Article ID 238075, 7 pages
doi:10.1155/2012/238075

Research Article

Lanthanum Influence on $EuAlO_3$ Perovskite Structural Properties: Experimental and Molecular Dynamics Studies

Enrique Lima,[1] María Elena Villafuerte-Castrejón,[1] José Saniger,[2] Victor Lara,[3] Jorge E. Sánchez-Sánchez,[4] and Luis Javier Álvarez[4]

[1] *Instituto de Investigaciones en Materiales, Universidad Nacional Autónoma de México, Circuito Exterior, A. P. 70-360, 04510 México, DF, Mexico*
[2] *CCADET, Universidad Nacional Autónoma de México, Circuito Exterior, A. P. 70-188, 04510 México, DF, Mexico*
[3] *Departamento de Química, Universidad Autónoma Metropolitana, Iztapalapa, Avenida San Rafael Atlixco No. 186, 09340 México, DF, Mexico*
[4] *Laboratorio de Simulación, Instituto de Matemáticas, Unidad Cuernavaca, Universidad Nacional Autónoma de México. AP-273-3 Admon. 3, Cuernavaca, Morelos 62251, Mexico*

Correspondence should be addressed to Enrique Lima, lima@iim.unam.mx

Received 13 September 2011; Revised 10 November 2011; Accepted 13 November 2011

Academic Editor: Peter Majewski

X-ray diffraction, ^{27}Al MAS NMR, and FTIR spectra along with results of molecular dynamics simulations were used to characterise $La_xEu_{1-x}AlO_3$ perovskites for $x = 0.3, 0.1$. Experimental and simulation results show that local changes in the perovskite-like structure can be achieved as lanthanum ions substitute europium ones. The introduction of La^{3+} ions in the $EuAlO_3$ parent causes an increase in the mobility of oxygen network.

1. Introduction

Various physical properties of $LaAlO_3$ as well as $EuAlO_3$ perovskites have both scientific and technological interest when doped with lanthanides [1, 2]. The 4f electrons of doping species are responsible for changes in their magnetic, electric, and optical properties. Rare earths containing perovskites have attracted attention mainly as semiconductor and/or optical materials [3–5]. A particularly interesting system that has not been thoroughly studied is the $La_{1-x}Eu_xAlO_3$ perovskite. In both parent perovskites, $LaAlO_3$, and $EuAlO_3$, aluminium cations are octahedrally coordinated and lanthanum and europium cations are located in dodecahedral sites [6, 7].

$La_{1-x}Eu_xAlO_3$ perovskites have been obtained through substitution of La^{3+} by Eu^{3+} in $LaAlO_3$ parent solid. These studies have been carried out previously and lattice parameters variations have been reported. However, these studies are limited to low percentages of substitution of La^{3+} by Eu^{3+} and were focused on the optical applications of these materials [8]. For instance, with the goal to maximize the fluorescence intensity on $La_{1-x}Eu_xAlO_3$, Klimke and Wulff studied the introduction of Eu^{3+} in a $LaAlO_3$ perovskite by solid-state reactions. They reported an optimal Eu^{3+} concentration of 1 mol% which is within the range of doping level for fluorescent materials [9]. However, diffusion of europium into perovskite lattice, induced by thermal treatment, is often restricted because microdomains of $EuAlO_3$ could appear. Then, samples with larger content of europium are prepared by chemical methods such as coprecipitation. Lanthanum is often used to stabilize perovskite-like catalysts [10] and europium due to its paramagnetic properties is used to modify the ionic conductivity of many perovskite-like materials [11]. Then, it is interesting to study lanthanum doping into $EuAlO_3$ because a more rigid structure could be obtained.

The crystalline structure of perovskite is expected to be preserved upon replacement of La^{3+} by Eu^{3+} given that Eu^{3+} can occupy the dodecahedral sites of La^{3+}. At low content of europium this assumption probably holds but at higher europium loadings the structure should be closer to

$EuAlO_3$ than $LaAlO_3$ structure. Besides, the differences of La^{3+} and Eu^{3+} regarding quadrupole and size could be important and cause alterations in the perovskite-like structure. Furthermore, La^{3+} and Eu^{3+} have very different electronic configurations, the first one has a configuration of noble gas (Xe) and the second one has a configuration $[Xe]4f^6$. These properties could be determinant to produce structural changes in the perovskite structure and of course can be used conveniently to tune the physicochemical properties of these materials. In order to investigate what happens upon a high percentage replacement of La^{3+} by Eu^{3+} in $LaAlO_3$, which should be equivalent to a low percentage replacement of Eu^{3+} by La^{3+} in $EuAlO_3$, we have studied the system $La_xEu_{1-x}AlO_3$ by applying a combination of experimental techniques of FTIR, XRD, and NMR and molecular dynamics simulations. Our results show how the introduction of La^{3+} produces strong modifications in the physical properties of the material, without significant changes in the structure as referred to that of $EuAlO_3$ perovskite.

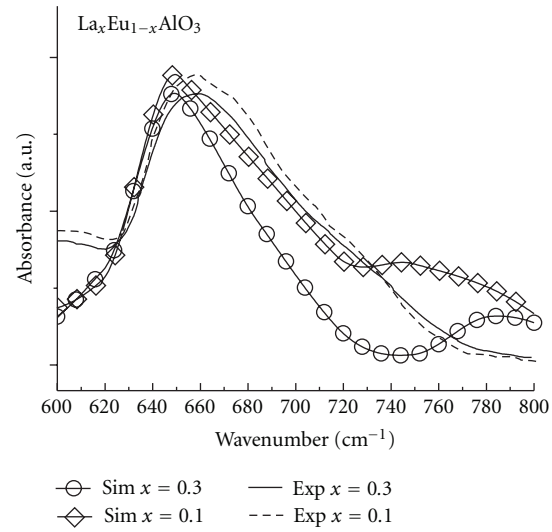

Figure 1: Infrared spectra, simulated and experimental, of perovskite samples with variable content of europium.

2. Experiments and Simulations

A series of $La_xEu_{1-x}AlO_3$ perovskites were synthesized by the coprecipitation method. Aqueous solutions of $La(NO_3)_2 \cdot 6H_2O$, $Al(NO_3)_3 \cdot 6H_2O$, and $Eu(NO_3)_3 \cdot 9H_2O$ with the desired La/Eu ratio were mixed and precipitated with NH_4OH. The precipitated solid was filtered in vacuum, washed with deionised water, and dried at 383 K. Finally, the solid was thermally treated twice, the first time at 973 K and the second one at 1673 K for 2 h and 6 h, respectively. Eu-containing perovskites were prepared with the following nominal composition: $LaAlO_3$, $La_{0.30}Eu_{0.70}AlO_3$, and $La_{0.10}Eu_{0.90}AlO_3$. Since there are not any sublimation phenomena to be expected we assumed the synthesis composition is the final one.

Powder X-ray diffraction (XRD) patterns were obtained using a D8 Advance Bruker AXS diffractometer, where a Cu target K_α ray ($\lambda = 0.154$ nm) was used as an X-ray source. Conventional identification of crystalline compounds was performed by comparing the diffractograms with JCPDS files (PDF card number 031-0022) [12]. Radial distribution functions, $g(r)$, were calculated from the full diffraction patterns as shown by Magini and Cabrini [13] which essentially consists of the Fourier transform of the structure factor S(k). A molybdenum anode X-ray tube was used to reach the required high values of the angular parameter $h = (4\pi \sin\theta)/\lambda$ and the X-ray pattern was measured by step scanning at angular intervals of 0.08° in a Siemens D5000 diffractometer. The cell parameters were obtained using a quartz standard to correct the shift of the (110) peak of the perovskite structure.

Solid-state ^{27}Al MAS NMR spectra were acquired under MAS conditions using an Avance 300 Bruker spectrometer with a magnetic field strength of 7.05 T, corresponding to a ^{27}Al Larmor frequency of 78.3 MHz. Short single pulses ($\pi/12$) and a recycle time of 0.5 s were used. The ^{27}Al chemical shift was referenced using an 1 M aqueous solution $Al(NO_3)_3$ as external standard.

For the infrared spectra (FTIR) all samples were diluted in CsI and then pressed to form pellets. Experiments were carried out at 2 cm^{-1} resolution and at room temperature using a Perkin-Elmer FTIR 2000 IR spectrometer and a DTGS Mid-IR detector.

Molecular dynamics simulations in the microcanonical ensemble were performed on two perovskite samples of composition $La_xEu_{1-x}AlO_3$, $x = 0.3,\ 0.1$. The interaction potential was of Pauling type given by

$$V\left(\vec{r}_{ij}\right) = \frac{q_i q_j}{r_{ij}} + \frac{e^2}{n\left(\sigma_i + \sigma_j\right)}\left(\frac{\sigma_i + \sigma_j}{r_{ij}}\right)^n, \qquad (1)$$

where q_i are the effective charges and σ_i are effective ionic radii. Charges were taken from reference [14] and long-range interactions were handled with Ewald sums. Since the local environment of Eu was not known at the beginning of the work the effective radius involved in the interaction potential had to be determined. In order to do so, we performed a series of MD simulations assigning different radii to particles representing Eu ions. One physical characteristic which depends on the ionic radius is the vibrational spectrum. The effective radius yielding the best fit to the IR spectrum for the concentration of Eu in the samples was $\sigma = 1.09$ Å which would correspond to a 6 coordinated Eu in the standard ionic radii data. Potential parameters used in the simulations are summarized in Table 1. Figure 1 shows the experimental and simulated IR spectra for $x = 0.3,\ 0.1$.

Simulation results were very similar for the two samples and therefore we constrain the report to the sample with $x = 0.7$. This simulated sample consisted of 2835 particles of which 567 represented Al ions, 1701 oxygen ions, 171 lanthanum ions, and 396 europium ions in an orthorhombic box of dimensions $a = 34.092$ Å, $b = 34.092$ Å, and $c = 26.516$ Å. The system was equilibrated at 300 K for 10 ps with temperature control previous to relaxation and production

Table 1: Potential parameters.

Atom	q, e	σ, Å
La	2.23	1.4
Eu	2.23	1.09
Al	1.92	0.67
O	−1.383	1.2

runs of 10 ps. In all runs, variations of total energy were of less than 0.01 per cent around the mean value, and temperature variations were of less than 2 K.

3. Results and Discussion

IR spectra were obtained to fit the interaction potential parameters. They presented only a single absorption band centered close to 655 cm^{-1}. The position of the IR absorption band moved to higher frequencies as the europium content increased. This shift to higher frequencies could be explained by the alteration of electrostatic interactions between ions. Europium and lanthanum cations have the same charge, however their masses and sizes are different and therefore there is a higher force constant for the system containing europium (La is ∼11% heavier than Eu, see Table 1 for radii).

Figure 2 shows the ^{27}Al MAS NMR spectra of samples $EuAlO_3$, $La_{0.3}Eu_{0.7}AlO_3$, and $LaAlO_3$. The spectrum of the europium-free sample, Figure 2(c), presents an isotropic narrow peak at 14 ppm which is assigned to sixfold coordinated aluminium in an oxygen environment [15], in agreement with the perovskite structure. The spectra of the europium content samples were very different to those of $LaAlO_3$ sample. Then, in order to find the position of the isotropic peak, the spectra acquired at variable spinning rate were performed (not shown); they have shown that in two europium-containing samples the isotropic peak is positioned at 213 ppm, Figure 2(a), 2(b). The NMR peak was significantly broader in $EuAlO_3$ than in $LaAlO_3$; of course this modification is mainly attributed to the electronic local environment created by europium introduction. Note that Eu^{3+} is a paramagnetic lanthanide ion that broads and shifts the NMR peak to down field. In spectrum of sample containing both europium and lanthanum, a shoulder close to 167 ppm and the small peak at 30 ppm suggest that lanthanum and europium are not homogeneously distributed into the perovskite structure, but some europium and lanthanum-rich domains could be formed. Interestingly, the NMR peak for sample $La_{0.3}Eu_{0.7}AlO_3$ is broader than in $EuAlO_3$ parent solid, suggesting that introduction of lanthanum modifies the distribution of charge and possibly a field electric gradient in this sample was created. This effect is discussed below in terms of the results of molecular dynamics simulations.

X-ray powder diffraction patterns confirm that all samples have a perovskite-like structure as can be observed from Figure 3. As lanthanum is incorporated to perovskite the cell parameter increases as can be seen from X-ray diffraction data in Figure 4. Table 2 shows the calculated cell parameters as a function of sample composition. This is attributed to the difference of La^{3+} and Eu^{3+} ionic radii. Note that even though

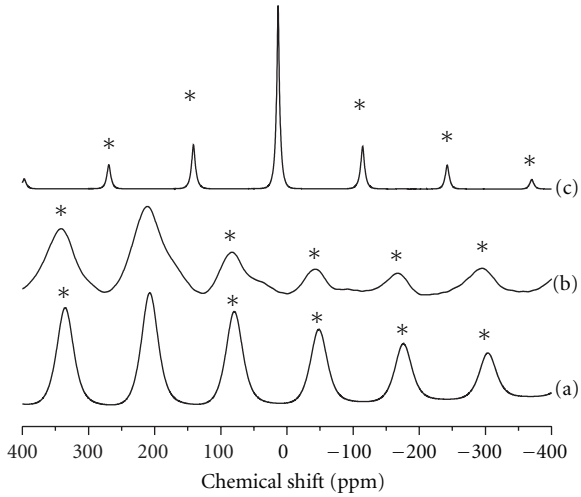

Figure 2: ^{27}Al MAS NMR spectra of $EuAlO_3$, $La_{0.30}Eu_{0.70}AlO_3$, and $LaAlO_3$; (a), (b), and (c), respectively. *indicates spinning side bands.

Table 2: Cell parameter of europium containing perovskites.

Sample	Cell parameter, a, Å
$LaAlO_3$	5.36
$La_{0.30}Eu_{0.70}AlO_3$	5.31
$La_{0.10}Eu_{0.90}AlO_3$	5.29
$EuAlO_3$	5.27

electrons in Eu^{3+} occupy f atomic orbitals, the cell parameter of $EuAlO_3$ is the lowest because the interstitial sites are determined by the oxygen packing and the ion-ion interactions.

Up to this point, experimental results show that lanthanum cations can replace europium cations in the parent $EuAlO_3$ perovskite. Even replacing as high as 30% Eu by La, XRD patterns show that the perovskite structure is preserved. NMR experiments, in addition, confirm that some local changes could have taken place when both lanthanum and europium are simultaneously present in perovskite structure. FTIR experiments also suggest some local changes as can be seen from the experimental curves, Figure 1. ^{27}Al MAS NMR results reveal that the local environment of aluminium is strongly altered. This modification could be attributed to electronic differences between europium and lanthanum. In fact La^{3+} is a diamagnetic species while, Eu^{3+} has non paired electrons promoting relaxation of NMR signal by paramagnetic effects which means that distances between aluminium and europium ions are short enough (in the second coordination sphere). It is not clear, however, what the consequences of this modification imply. Actually, short distances between aluminum and europium appear because of the subtle distortion of the lattice produced by heavy doping with Eu. The lattice distortions, however, are not so great that coordination of cations could occur in other complex perovskites [16]. Molecular dynamics (MD) allows for the elucidation of very subtle changes in some characteristics of

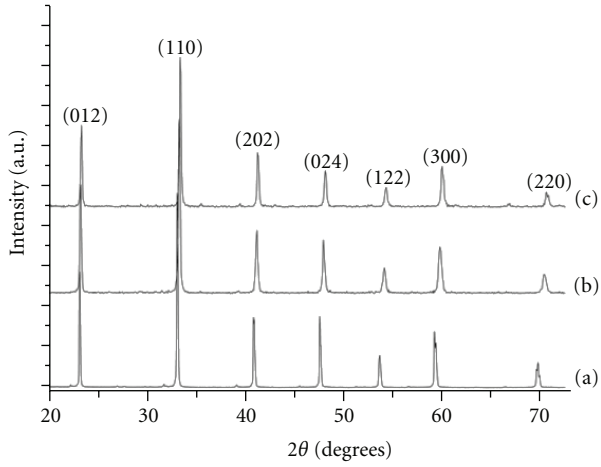

FIGURE 3: XRD patterns of (a) $LaAlO_3$, (b) $La_{0.3}Eu_{0.7}AlO_3$, and (c) $La_{0.1}Eu_{0.9}AlO_3$. Perovskite-like structure is maintained although a small change in cell parameter a is observed. Peaks are indexed with PDF card number 031-0022.

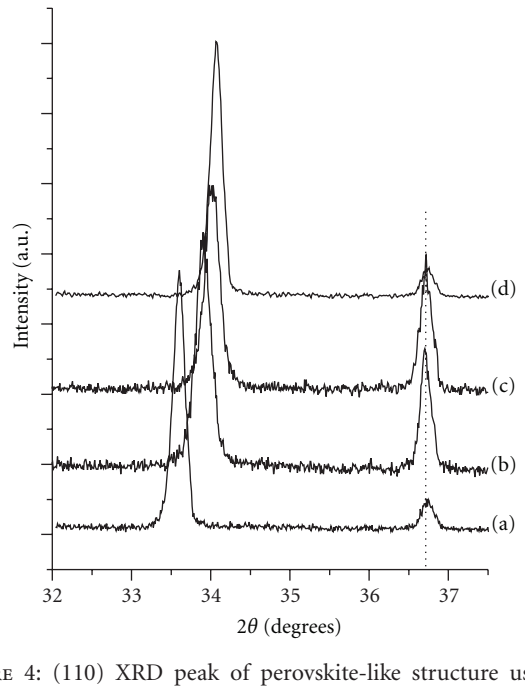

FIGURE 4: (110) XRD peak of perovskite-like structure used to calculate the cell parameters of (a) $LaAlO_3$, (b) $La_{0.3}Eu_{0.7}AlO_3$, (c) $La_{0.1}Eu_{0.9}AlO_3$, and (d) $EuAlO_3$. As standard, the peak of quartz was used (marked with the dotted line).

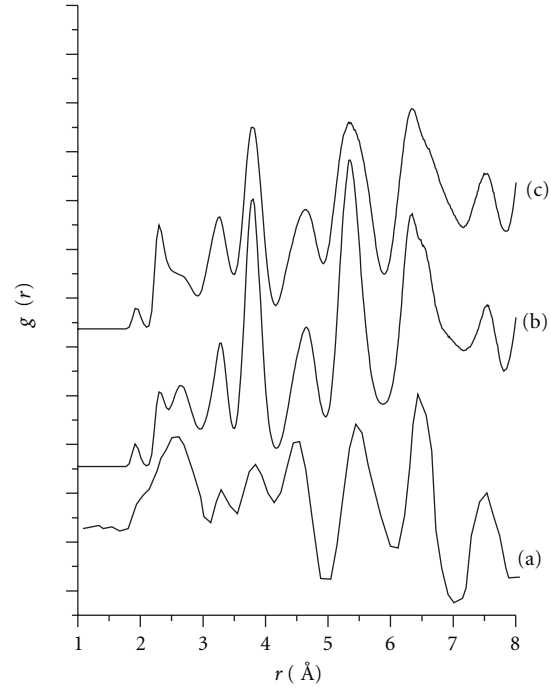

FIGURE 5: Radial distribution functions from experimental (a) and molecular dynamics simulations (b and c); $La_{0.3}Eu_{0.7}AlO_3$ (a), $La_{0.3}Eu_{0.7}AlO_3$ (b), and $La_{0.1}Eu_{0.9}AlO_3$ (c).

microscopic systems. Figure 5 shows the total radial distribution functions, $g(r)$, of europium-containing perovskites calculated from MD simulations. Even though some peaks are difficult to resolve experimentally, the rough agreement between simulated and experimental data is fairly good as far as the position of the peaks and the general shape of the functions is concerned. Some features of the radial distribution functions are (1) the peak at 2.6 Å increases as europium content increases; (2) peaks between 5 and 8 Å go to longer distances as lanthanum content increases; (3) the peak at 1.9 Å, due to Al–O distances, remains constant in intensity and position. This last observation implies that octahedral coordination of aluminium ions is not altered or its alteration is very subtle as a consequence of replacement of europium by lanthanum. Therefore, the observed changes in ^{27}Al NMR spectra are mainly due to differences in electronic properties of La^{3+} and Eu^{3+} ions. In addition, as mentioned above, lanthanide ions are heterogeneously distributed into the perovskite structure.

The structural effects of the presence of La^{3+} and Eu^{3+} in the perovskite lattice can be described in some detail from the partial radial distribution functions, $g(r)$. Figure 6 shows the Al–O, La–O, Al–Al, and O–O pair functions for the simulated $LaAlO_3$, $La_{0.3}Eu_{0.7}AlO_3$, and $EuAlO_3$ samples. The first neighbour distances Al–O and La–O are very well defined and are unchanged upon substitution as can be seen from the figure. The three La–O first neighbour bond distances are a bit more differentiated in the sample with europium as can be noted from the asymmetry of the first peak. A coordination analysis performed after the molecular dynamics runs yielded the same coordination numbers for both samples Al (6) and La or Eu (12). It can be noted that all other peaks broaden implying that long-range order is not totally preserved. Note that the second peak of $g(r_{AlO})$ splits in two peaks upon the presence of europium in perovskites. This may be interpreted in terms of the AlO_6 octahedron tilting known to appear in $ABXO_3$ perovskites. Upon heavy doping with Eu a more complex tilting may occur that produces a lowering of symmetry and is reflected in this second peak of $g(r_{AlO})$. On the other hand,

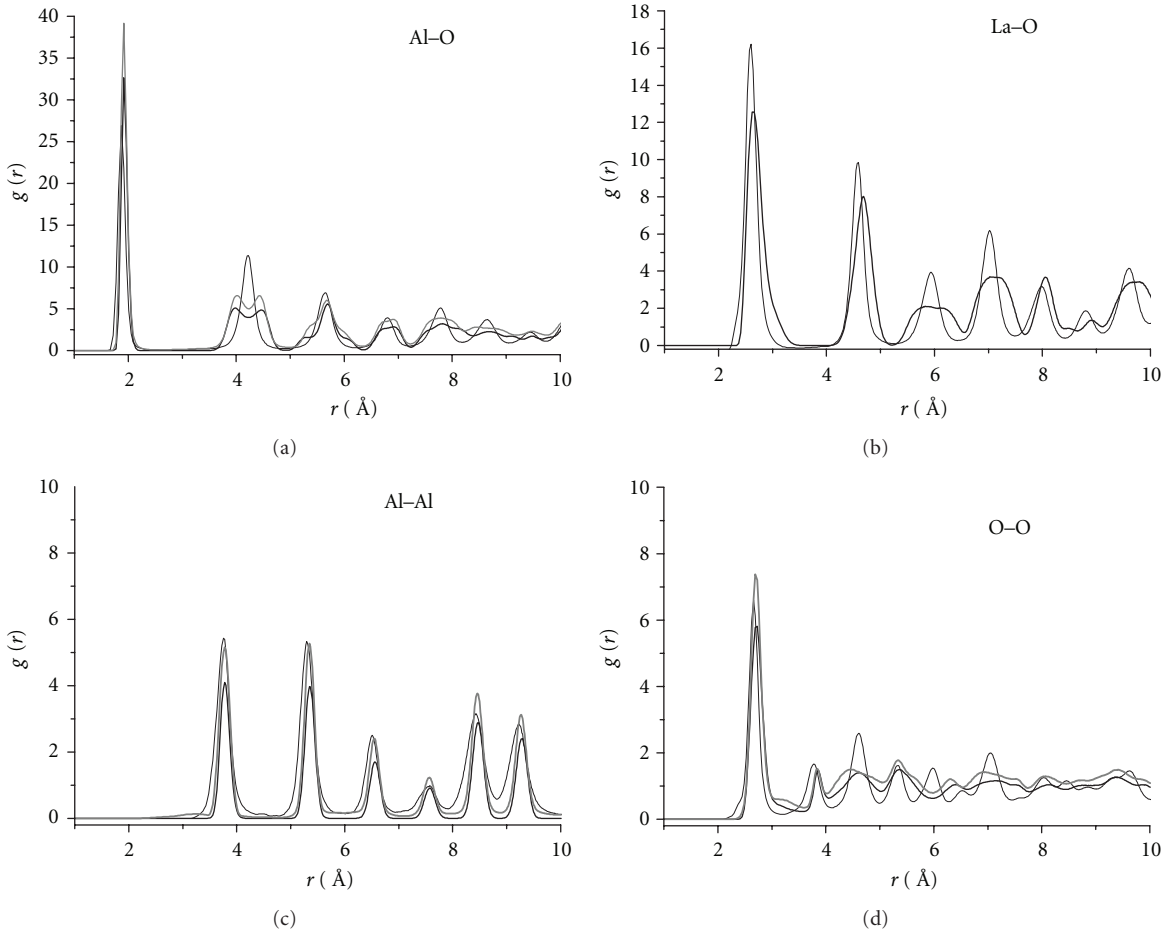

Figure 6: Radial distribution functions from molecular dynamics simulations for the pairs shown for samples $LaAlO_3$ (black thin line), $La_{0.3}Eu_{0.7}AlO_3$ (black line), and $EuAlO_3$ (gray line).

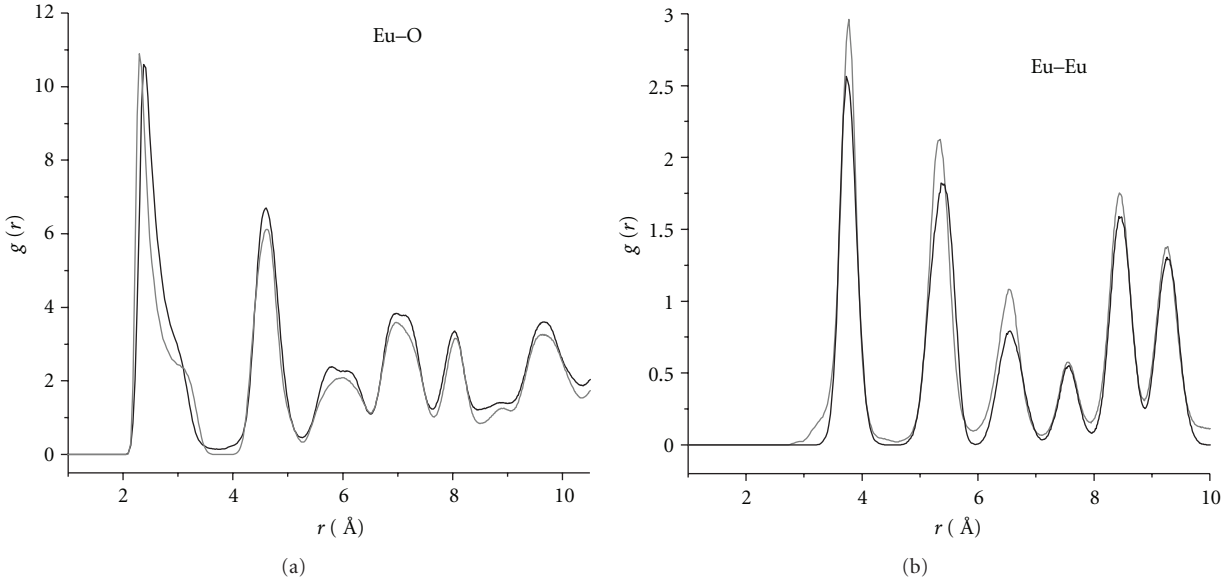

Figure 7: Radial distribution functions from molecular dynamics simulations for the pairs shown for samples $La_{0.3}Eu_{0.7}AlO_3$ (black line) and $EuAlO_3$ (gray line).

the aluminium sublattice remains practically unaltered upon substitution, as it can be seen from $g(r_{\mathrm{AlAl}})$. Finally, an interesting conclusion is derived from the O–O partial radial distribution function, $g(r_{\mathrm{OO}})$, since a remarkable broadening of peaks is presented from 4 Å on samples containing Eu, shown in Figure 6. This implies a constant rearrangement of oxygen atoms in such a way that in the long range they appear as disordered. This is shown by the O–O $g(r)$ asymptotic trend to unity. This means that in the real world the presence of Eu^{3+} significantly increases the entropy. From a purely classical mechanics point of view, one can interpret these effects as due to the fact that europium is about 11% heavier than lanthanum; therefore for a given temperature, oxygen atoms in the vicinity of europium increase the amplitude of their vibrations. If oxygen vibrations increase in amplitude and therefore if average oxygen atoms are not at the crystalline positions, the energy activation barriers for diffusion processes either disappear or else are lowered in a significant way.

Figure 7 displays the $g(r_{\mathrm{EuO}})$ and $g(r_{\mathrm{EuEu}})$ functions, confirming that europium sublattice is also preserved and only the position of oxygen ions changes, modifying then the distances at first neighboring Eu–O.

Factors governing the electrical ionic conductivity of perovskites are concentration of oxygen vacancies, oxygen partial pressure, crystal structure, and defects, among others [17–19]. Our findings indicate that even in the absence of defects, such as oxygen vacancies, one important factor that may substantially change the ionic conductivity is the increase of oxygen mobility if the proper cation is introduced in the perovskite network.

4. Conclusions

We have performed a structural analysis of La^{3+}-doped $EuAlO_3$. Molecular dynamic simulations, as well as ^{27}Al MAS NMR spectra analysis, indicates that coordination of cations in the doped sample remains the same as in the parent perovskite. Since substitution of La by Eu is isomorphic, no O vacancies are generated. The only structural change observed is that the oxygen sublattice gains rigidity because of the decrease of oxygen vibration amplitude.

Acknowledgments

Thanks are due to G. Cedillo and A. Tejeda (IIM-UNAM) for the technical help. The authors thank PAPIIT-UNAM (IN107110) for financial support. All calculations were carried out on an IBM SP3 supercomputer kindly donated to Laboratorio de Simulación of Instituto de Matemáticas, Unidad Cuernavaca, UNAM by Fundación Clínica Médica Sur, A. C. from Mexico City.

References

[1] J. B. A. A. Elemans, B. Van Laar, K. R. Van Der Veen, and B. O. Loopstra, "The crystallographic and magnetic structures of $La_{1-x}Ba_xMn_{1-x}Me_xO_3$ (Me = Mn or Ti)," *Journal of Solid State Chemistry*, vol. 3, no. 2, pp. 238–242, 1971.

[2] J. Mizusaki, I. Yasuda, J. I. Shimoyama, S. Yamauchi, and K. Fueki, "Electrical conductivity, defect equilibrium and oxygen vacancy diffusion coefficient of $La_{1-x}Ca_xAlO_{3-\delta}$ single crystals," *Journal of the Electrochemical Society*, vol. 140, no. 2, pp. 467–471, 1993.

[3] Y. H. Huang, S. Wang, F. Luo, S. Jiang, and C. H. Yan, "Enhanced magnetoresistance at high temperatures in $La_{0.7}Sr_{0.3}MnO_3$/silica nanocomposites," *Chemical Physics Letters*, vol. 362, no. 1-2, pp. 114–118, 2002.

[4] G. Thornton, B. C. Tofield, and A. W. Hewat, "A neutron diffraction study of $LaCoO_3$ in the temperature range 4.2 < T < 1248 K," *Journal of Solid State Chemistry*, vol. 61, no. 3, pp. 301–307, 1986.

[5] M. Yashima, M. Mori, T. Kamiyama et al., "High-temperature phase transition in lanthanum titanate perovskite $La_{0.64}(Ti_{0.92},Nb_{0.08})O_3$," *Chemical Physics Letters*, vol. 375, no. 1-2, pp. 240–246, 2003.

[6] R. M. Hazen, "A useful fiction: Polyhedral modeling of mineral properties," *American Journal of Science*, vol. 74, pp. 242–269, 1988.

[7] A. R. West, *Solid State Chemistry and Its Application*, John Wiley & Sons, New York, NY, USA, 1990.

[8] D. Hreniak, W. Stręk, P. Dereń, A. Bednarkiewicz, and A. Łukowiak, "Synthesis and luminescence properties of Eu^{3+}-doped $LaAlO_3$ nanocrystals," *Journal of Alloys and Compounds*, vol. 408–412, pp. 828–830, 2006.

[9] J. Klimke and H. Wulff, "Determination of the optimum Eu^{3+}-concentration in $LaAlO_3$: euphosphors by X-ray diffraction and fluorescence measurements," *Fresenius' Journal of Analytical Chemistry*, vol. 349, no. 1–3, pp. 245–246, 1994.

[10] J. L. Hueso, A. Caballero, J. Cotrino, and A. R. González-Elipe, "Plasma catalysis over lanthanum substituted perovskites," *Catalysis Communications*, vol. 8, no. 11, pp. 1739–1742, 2007.

[11] M. M. Seikh, V. Caignaert, V. Pralong, C. Simon, and B. Raveau, "Expansion of ferromagnetism by calcium doping in the ordered oxygen deficient perovskite $EuBaCo_2O_{5.50\pm\delta}$," *Journal of Physics Condensed Matter*, vol. 20, no. 1, Article ID 015212, 2008.

[12] Join Committee on Powder Diffraction Standards JCPDS Files, International Center for Diffraction Data, 2000.

[13] M. Magini and A. Cabrini, "Programme en FORTRAN IV pour l'analyse des données expérimentales relatives à la diffusion des rayons X par des substances liquides, amorphes et microcristallisées," *Journal of Applied Crystallography*, vol. 5, pp. 14–18, 1972.

[14] L. J. Alvarez, J. F. Sanz, M. J. Capitán, and J. A. Odriozola, "Onset of perovskite formation in the catalytic system $La_2O_{3/\gamma}$-Al_2O_3," *Catalysis Letters*, vol. 21, no. 1-2, pp. 89–97, 1993.

[15] E. Lippmaa, A. Samoson, and M. Mägi, "High-resolution ^{27}Al NMR of aluminosilicates," *Journal of the American Chemical Society*, vol. 108, no. 8, pp. 1730–1735, 1986.

[16] V. I. Torgashev, V. B. Shirokov, A. S. Prokhorov, and L. A. Shuvalov, "Competition between rotational and polar structural distortions in perovskites," *Crystallography Reports*, vol. 50, no. 4, pp. 637–645, 2005.

[17] B. P. Burton, "Long-range versus short-range interactions and the configurational energies of $Ba(B,B')O_3$ and $Pb(B,B')O_3$ perovskites," *Modelling and Simulation in Materials Science and Engineering*, vol. 8, no. 3, pp. 211–219, 2000.

[18] T. L. Nguyen, M. Dokiya, S. Wang, H. Tagawa, and T. Hashimoto, "The effect of oxygen vacancy on the oxide ion

mobility in $LaAlO_3$-based oxides," *Solid State Ionics*, vol. 130, no. 3-4, pp. 229–241, 2000.

[19] E. Lima, M. E. Villafuerte-Castrejon, J. M. Saniger, A. Ibarra-Palos, J. E. Sanchez-Sanchez, and L. J. Álvarez, "Experimental XRD and NMR, and molecular dynamics study of Sr containing $LaAlO_3$ perovskite," *Solid State Ionics*, vol. 178, no. 39-40, pp. 1944–1949, 2008.